Essential Role of Tyrosine 229 of the Oxaloacetate Decarboxylase β-Subunit in the Energy Coupling Mechanism of the Na^+ Pump†

Petra Jockel,‡ Markus Schmid,‡ Thomas Choinowski,§ and Peter Dimroth*,‡

Institut für Mikrobiologie der Eidgenössischen Technischen Hochschule, ETH-Zentrum, CH-8092 Zürich, Switzerland, Institut für Biochemie der Eidgenössischen Technischen Hochschule, ETH-Zentrum, CH-8092 Zürich, Switzerland

Received December 8, 1999; Revised Manuscript Received January 27, 2000

ABSTRACT: The membrane-bound β-subunit of oxaloacetate decarboxylase from *Klebsiella pneumoniae* catalyzes the decarboxylation of carboxybiotin, which is coupled to Na^+ translocation and consumes a periplasmically derived proton. Upon site-directed mutagenesis of 20 polar and/or conserved residues within putative membrane-integral regions, the specific oxaloacetate decarboxylase activities were reduced to various extents, but only the enzyme with a Y229F mutation was completely inactive. We propose that Y229 is part of the network by which the proton of S382 is delivered to carboxybiotin, where it is consumed upon catalyzing the immediate decarboxylation of this acid-labile compound. Unlike S382 or D203, Y229 appears to be not involved in Na^+ binding, because in the Y229F orY229A mutants, the β-subunit was protected from tryptic digestion by 50 mM NaCl like in the wild-type enzyme. Oxaloacetate decarboxylase with a βC291E mutation was unstable in the absence of Na^+ and dissociated into an $\alpha-\gamma$ subcomplex and the β-subunit. The enzyme could only be isolated in the presence of 0.5 M NaCl. These results are consistent with the notion that the β-subunit changes its conformation upon Na^+ binding.

Oxaloacetate decarboxylase of *Klebsiella pneumoniae* is the paradigm for the sodium ion translocating decarboxylases, an enzyme family that also includes methylmalonyl-CoA decarboxylase, glutaconyl-CoA decarboxylase, and malonate decarboxylase (*1*−*3*). The *oadGAB* genes encode subunits γ, α, and β (OadG, A, and B) of oxaloacetate decarboxylase (*4*−*6*) and are part of the citrate fermentation gene cluster. This cluster, which has been thoroughly characterized in *K. pneumoniae*, also includes the genes for citrate lyase, a Na^+-dependent citrate carrier and a two component regulatory system (*7*−*9*). The derived proteins are specifically required for the anaerobic growth on citrate.

Organization and function of the three subunits of oxaloacetate decarboxylase are illustrated in Figure 1. The α-subunit is a peripheral membrane protein, harboring the carboxyltransferase activity in the N-terminal domain and the biotin-carrier-function in the C-terminal domain (*4*, *10*). The β-subunit is an integral membrane protein, composed of nine transmembrane α-helices, a hydrophobic segment inserting into the membrane from the periplasmic surface in an undefined manner (region IIIa), and connecting loops of various lengths [Figure 2 (*11*)]. The β-subunit catalyzes the decarboxylation of carboxybiotin bound to OadA, which is coupled to Na^+ pumping and consumes a periplasmically derived proton (*1*, *12*). The γ-subunit has a membrane anchor in its N-terminal part and a hydrophilic C-terminal portion

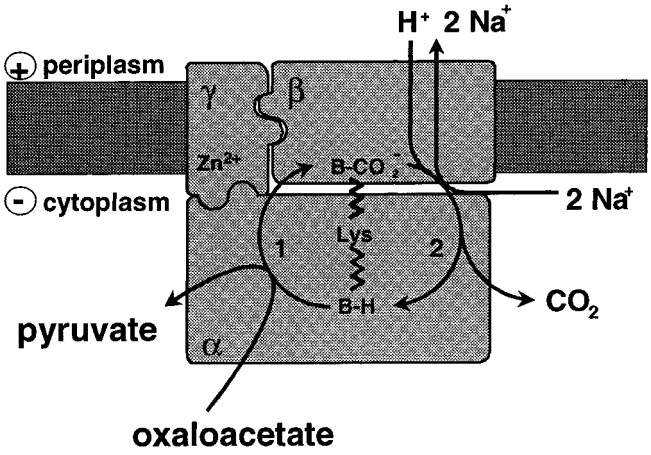

FIGURE 1: Cartoon showing the overall geometry of the oxaloacetate decarboxylase and features of the catalytic events. B−H, biotin; $B-CO_2^-$, carboxybiotin; Lys, biotin-binding lysine residue; (1) carboxyltransferase reaction and (2) decarboxylase reaction.

with an attached Zn^{2+} metal ion (*12*, *14*). The γ-subunit keeps the complex together, and it accelerates the carboxyltransfer reaction, presumably by polarizing the carbonyl oxygen bond of oxaloacetate with its Zn^{2+} ion (*14*).

The most highly conserved portions of OadB are region IIIa in the vicinity of the invariable D203 residue and transmembrane helix VIII. Mutational analyses indicated that D203 and the helix VIII residues, S382 and G377, are essential not only for Na^+ translocation but also for the decarboxylation of carboxybiotin (*12*, *15*). Other residues of functional significance are N373 and R389 of helix VIII. It was proposed that the D203/N373 pair forms a Na^+-binding site near the periplasmic surface and that a second Na^+-binding site is located at S382 in the center of the bilayer

† This work was supported by Swiss National Science Foundation.
* To whom correspondence should be addressed. Phone: 0041 1 632 33 21. Fax: 0041 1 632 13 78. E-mail: dimroth@micro.biol.ethz.ch.
‡ Institut für Mikrobiologie der Eidgenössischen Technischen Hochschule.
§ Institut für Biochemie der Eidgenössischen Technischen Hochschule.

10.1021/bi992817e CCC: $19.00
Published on Web 03/21/2000

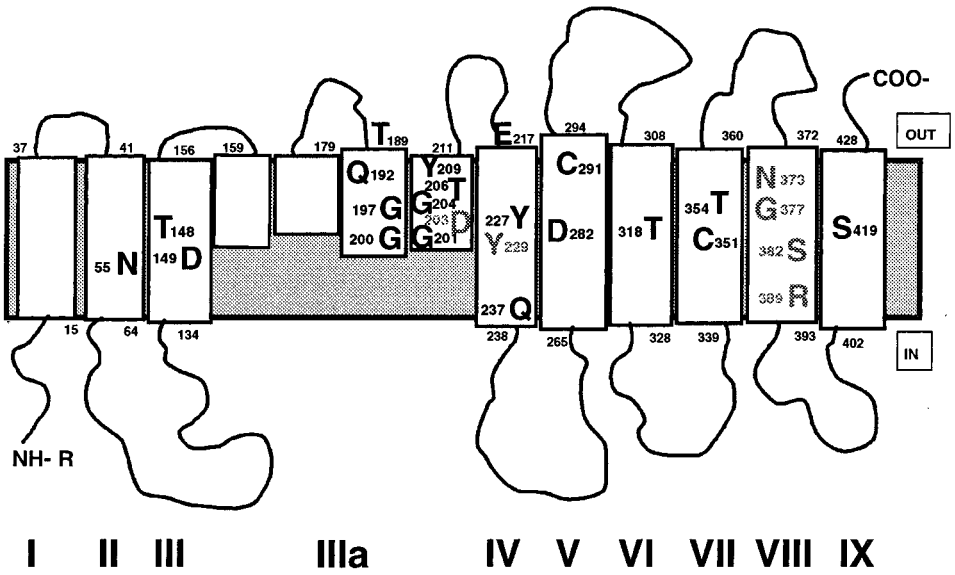

FIGURE 2: Topology model of the β-subunit of the oxaloacetate decarboxylase showing functionally important amino acid residues in gray. Those mutagenized residues which led to functionally intact oxaloacetate decarboxylases are indicated in black.

(*15*). A possible mechanism involves binding of carboxybiotin near R389 and of two cytoplasmically derived Na^+ ions to the two binding sites. It was proposed that binding of Na^+ to S382 displaces a proton, which moves via R389 to the carboxybiotin, thereby catalyzing the decarboxylation of this acid-labile compound. The decarboxylation is suggested to trigger a conformational change, by which the Na^+ ions become exposed toward the periplasmic surface and dissociate. Simultaneously, a proton entering the channel from the periplasm reforms the hydroxyl group of S382. Rebinding of carboxybiotin switches OadB back to the original conformation, and a new catalytic cycle begins (*15*).

In this study, we have selected additional conserved amino acid residues of OadB for site-specific mutagenesis. In all of these mutants, the oxaloacetate decarboxylase activity was reduced to various extents. The most conspicuous results were obtained with mutants of Y229, defining this residue as crucial for the catalytic mechanism.

EXPERIMENTAL PROCEDURES

Bacterial Strains. The bacterial strains *Escherichia coli* DH5α (Bethesda Research Laboratories), *E. coli* JM110 (*16*), *E. coli* EP432 (*17*), and *E. coli* BL21(DE3)pLysS (*18*) were used in this study. All strains, except *E. coli* EP432, were grown at 37 °C in Luria Bertani (LB) medium (*19*). *E. coli* EP432 was grown as described (*15*). Plasmid-containing strains were supplemented with the selective antibiotics ampicillin (100 μg/mL) and/or chloramphenicol (40 μg/mL) or kanamycinsulfate (50 μg/mL). *K. pneumoniae* was the source for plasmid pSK-GAB harboring the genes for the oxaloacetate decarboxylase (*14*).

Recombinant DNA Techniques. Standard recombinant DNA techniques were performed essentially as described by Sambrook et al. (*19*). Polymerase chain reactions (PCRs)[1] were performed using Vent-DNA-Polymerase from New England Biolabs (Beverly, MA). DNA sequencing was carried out according to the dideoxynucleotide chain-termination method (*20*) using a *Taq* DyeDeoxy terminator cycle kit and the ABI Prism 310 genetic analyzer from Applied Biosystems.

Construction of Site-Directed Mutants of the β-Subunit. The primers used for site-directed mutagenesis are listed in Table A of Supporting Information. Site-directed mutants were obtained as follows. The PCR fragments containing the mutations were constructed in a two-step protocol. For the N-terminal part of the PCR fragments of the β-subunit, primer prN or prBN and primers with the affix *rev* were used, and pSK-GAB (*14*) served as template. For the corresponding PCR fragments of the C-terminal part of the β-subunit, primers prC or prBC and primers with the affix *for* were used, and pSK-GAB (*14*) served as template. After purification, those PCR fragments were used as template for the PCR products from primers prN and prC or primers prBN and prBC, which contained the mutation. PCR fragments were digested with *Kpn2*I and *Bcl*I, in case of fragments from primers prN and prC, or with *Bcl*I and *Bst1107*I, in case of fragments from primers prBN and prBC and cloned into pSK-GAB. From pSK-GAB, which was isolated from JM110 cells, the *Kpn2*I/*Bcl*I or *Bcl*I/*Bst1107*I fragment was removed.

Purification of Oxaloacetate Decarboxylase Variants and Enzyme Assays. Mutant oxaloacetate decarboxylases were purified from *E. coli* DH5α/pSK-GAB variants by affinity chromatography of a solubilized membrane extract on a SoftLink monomeric avidin-Sepharose column (Promega) (*21*). Large-scale purification was performed as described previously (*14*). The decarboxylation activity was determined with the simple spectrophotometric assay at 265 nm (*21*).

Screening of Oxaloacetate Decarboxylase Activity from Mutant Clones. Before a large-scale purification of the mutant protein was performed, a small-scale culture of the respective clone was used to measure oxaloacetate decarboxylase activity (*12*). To check for an active Na^+ pump, the mutant plasmid was transformed into *E. coli* EP432, which lacks both Na^+/H^+ antiporters, and the growth on a glucose mineral medium was determined in the presence of 360 mM NaCl. Such growth is only observed if the Na^+

[1] Abbreviations: PCR, polymerase chain reaction; SDS, sodium dodecyl sulfate; SDS−PAGE, sodium dodecyl sulfate−polyacrylamide gel electrophoresis.

pump is functional (*15*).

Labeling of Oxaloacetate Decarboxylase and Mutant Enzymes with $^{14}CO_2$ from [4-^{14}C]Oxaloacetate. [4-^{14}C]-Oxaloacetate, prepared from [4-^{14}C]L-aspartate and 2-oxoglutarate with glutamate:oxaloacetate transaminase, was used to measure the transfer of the radioactive carboxyl residue from [4-^{14}C]oxaloacetate to the biotin bound to OadA, as described (*15*).

Determination of Oxaloacetate Decarboxylase Activity at Various Na^+ Concentrations and pH Values. The decarboxylation activities of wild-type (DH5α/pSK-GAB) and mutant oxaloacetate decarboxylases were measured at pH values ranging between pH 5.5 and 8.8, in 40 mM Mes/Tris buffer, containing variable Na^+ concentrations, utilizing the simple spectrophotometric assay (*21*).

Analytical Procedures. The protein content of samples was determined according to Bradford (*22*) or by the bicinchoninic acid method (*23*).

Effect of Na^+ on Tryptic Hydrolysis of the Oxaloacetate Decarboxylase β-Subunit. Protection from proteolytic digestion of the β-subunit by Na^+ ions was determined for the mutants Y227A, Y227F, Y229A, Y229F, and C291E. The incubation mixtures contained in 60 μL at 25 °C were as follows: (A) 20 mM potassium phosphate buffer, pH 7.5, 50 mM potassium chloride, purified wild-type or mutant oxaloacetate decarboxylase (25 μg) and 3 μg of trypsin; a parallel incubation mixture (B) contained 50 mM sodium chloride instead of potassium chloride. Samples (12 μL) were transferred after 0 (before adding of trypsin), 2, 4, 7.5, and 24 h incubation into 1 μL of 50 mM phenylmethanesulfonyl fluoride and 12 μL of SDS sample buffer to stop proteolysis. The samples were subsequently analyzed by SDS−PAGE and the halftime for tryptic digestion of the β-subunit was determined. (*15*).

Molecular Modeling. Molecular modeling of the active-site domain in the β-subunit of oxaloacetate decarboxylase was performed on a Silicon Graphics INDIGO 2 workstation with the program CHAIN (*24*). The three-dimensional model of the two transmembrane helices IV and VIII was built using α-helical polyalanine segments consisting of 20 residues. These alanines were then transformed into the corresponding side chains according to the primary sequence (*5*, *6*). Helices IV and VIII, having an extension of about 29 Å, were positioned within van der Waals contact distances parallel to each other. The atomic coordinates of a biotin from the biotin-binding protein avidin [Brookhaven Protein Data Bank code , 1AVD (*25*)] were used as a template to generate the carboxybiotin.

RESULTS

Selection of Amino Acids for Site-Directed Mutagenesis. The oxaloacetate decarboxylase β-subunit consists of 433 residues, of which 59 are conserved among eight related proteins (*15*). These and a few others with conservative exchanges are the only ones that could be of functional relevance. Site-directed mutagenesis could therefore be restricted to these residues. We further reasoned that conserved polar residues in transmembrane helices are the key candidates to participate in ion binding and translocation, and we therefore selected them for mutagenesis first. Conserved glycines were included, since they might be well suited to align channel-like portions within the molecule due to their lacking side chains or they might be located at critical interhelix connections. With this approach, we have already identified D203 of region IIIa and N373, G377, S382, and R389 of helix VIII as residues with functional importance for decarboxylation-coupled Na^+ translocation across the membrane (*12*, *15*). Twenty additional amino acids of the category described above have now been mutagenized and characterized. All mutated amino acids are highlighted in Figure 2.

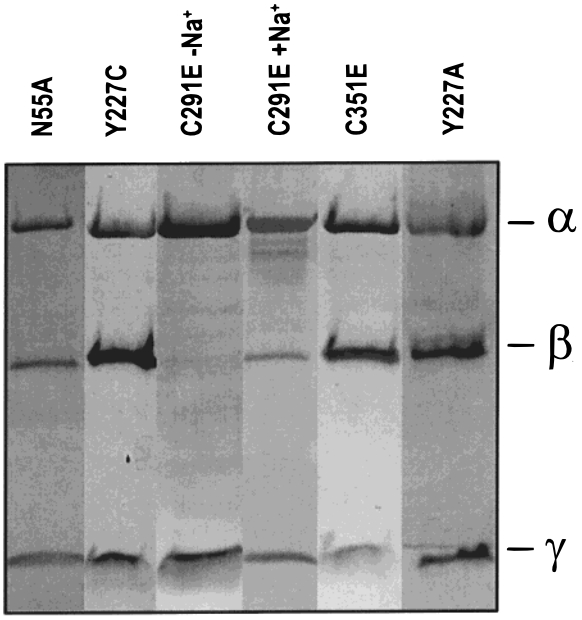

FIGURE 3: Expression of mutant oxaloacetate decarboxylases as evidenced from silver-stained SDS−PAGE after purification of the proteins. Mutations in OadB are indicated. α, β, and γ denote the three subunits of oxaloacetate decarboxylase. Oxaloacetate decarboxylase with the C291E mutation was isolated in the absence of Na^+ (C291E − Na^+) or in the presence of 0.5 M NaCl (C291E + Na^+).

Synthesis of Mutant Oxaloacetate Decarboxylases in E. coli and specific activities of the mutant enzymes. To synthesize the mutant oxaloacetate decarboxylases, mutated DNA fragments were cloned into pSK-GAB (*14*) using appropriate restriction sites, and used to transform *E. coli* DH5α, as described in Experimental Procedures. Grown cells were disrupted, and the oxaloacetate decarboxylases were purified by affinity chromatography of solubilized membrane fractions (*21*). Synthesis of the three subunits of the decarboxylases was verified for all mutants described here by sodium dodecyl sulfate−polyacrylamide gelelectrophoresis (SDS−PAGE), and a selection of these results is shown in Figure 3. Expression of mutant enzymes was quantified by protein determination. These results are given in Table 1 together with the specific activities of the isolated mutant enzymes. Between 0.05 and 0.6 mg/g cells of the oxaloacetate decarboxylase variants could be isolated. In most of these mutants, the specific oxaloacetate decarboxylase activity dropped to a range between 5 and 54% of the wild-type enzyme. The corresponding amino acids contribute, therefore, to a high specific activity of the decarboxylase, but are not absolutely essential for function. The most severe effects on activity were observed by mutating tyrosines 227 and 229 in transmembrane helix IV. In the Y227A mutant, the specific activity dropped to 0.5 units/mg protein compared

Table 1: (A) Synthesis of Mutant Oxaloacetate Decarboxylases from OadB Variants and Specific Activities of Isolated Enzymes; (B) Growth of *E. coli* EP432 Transformed with Plasmids Expressing Mutant Oxaloacetate Decarboxylases on Glucose Mineral Medium in the Presence of 360 mM NaCl

	A		B
mutation	amount of oxaloacetate decarboxylase isolated (mg/g wet packed cells)[a]	specific activity (units/mg)	optical density at 600 nm[b]
wild-type	0.5	45	0.5
N55A	0.6	20	0.4
T148A	0.5	4	0.4
T189A	0.3	18	0.4
Q192L	0.1	2	0.4
G197A	0.3	8	0.5
G200A	0.3	5	0.4
G201A	0.3	10	0.4
G204A	0.2	7	0.4
T206A	0.3	20	0.4
Y209A	0.05	3	0.3
E217A	0.4	6	0.4
Y227A	0.4	0.5	0
Y227C	0.3	12	0.3
Y227F	0.1	9	0.4
Y229A	0.2	0.02	0
Y229F	0.1	0	0
Q237A	0.2	8	0.5
D282A	0.3	24	0.4
C291E	0.2	4	0.4
T318A	0.5	12	0.4
C351E	0.2	3	0.3
T354A	0.2	3	0.4
S419A	0.1	4	0.4

[a] From *E. coli* DH5α/pSK GAB containing the mutation indicated. [b] Growth of *E. coli* EP432 containing plasmid pSK GAB with the mutation indicated. The optical density was determined after 28 h growth at 30 °C.

to 45 units/mg for the wild-type, but the Y227C or Y227F variants had specific activities of around 10 units/mg protein. Hence, a tyrosine at position 227 ensures high specific activity of the oxaloacetate decarboxylase but is not essential for the function of the enzyme. The oxaloacetate decarboxylase activity was completely abolished upon mutating Y229 to F and below 0.1% of the wild-type activity was found in the Y229A mutant. Therefore, for Y229, we envisage a crucial role in the decarboxylation mechanism (see Discussion).

Oxaloacetate decarboxylase with a βC291E mutation retained 8% of the wild-type specific activity. An interesting phenotype of this mutant was a severe reduction of the stability of the enzyme complex in the absence of Na^+. If Na^+ was omitted, an $\alpha-\gamma$ subcomplex was purified by avidin-Sepharose affinity chromatography, but in the presence of 0.5 M NaCl, the $\alpha-\beta-\gamma$ complex was obtained (Figure 3). These results are consistent with the notion that Na^+ binding induces a conformational change of the β-subunit (*3*, *13*, *27*). This change in the conformation was further corroborated by the protection of the β-subunit with the C291E mutation from tryptic hydrolysis in the presence of 50 mM NaCl with characteristics similar to those of the wild-type enzyme (Table 3).

Formation of Stable Carboxybiotin Enzyme Derivatives with Mutants in OadB, Which Are Inactive in Oxaloacetate Decarboxylation. The first step in oxaloacetate decarboxylation is the transfer of the carboxyl group from oxaloacetate to the biotin prosthetic group (*26*). This reaction is catalyzed by OadA and was therefore not affected by the βY229F mutation, as shown by the formation of the [^{14}C]carboxybiotin enzyme derivative upon incubation of the mutant with [4-^{14}C]oxaloacetate (Table 2). As the subsequent decarboxylation was impaired, sodium ions were without effect on the labeling of the enzyme. In contrast, stable carboxybiotin enzyme derivatives were not obtained for the Y227A or Y229A mutants, which have low residual oxaloacetate decarboxylase activities (Table 1). We conclude, therefore, that the carboxybiotin decarboxylase activity was abolished in the Y229F mutant and that this activity was significantly affected but not impaired in the Y227A or Y229A mutants.

Table 2: Formation of [^{14}C]Carboxybiotin Enzyme Derivatives by Carboxyltransfer from [4-^{14}C]Oxaloacetate to Mutants in OadB, Which Are Inactive or Nearly Inactive in Oxaloacetate Decarboxylation[a]

mutation	amount of enzyme (μg)	protein-bound radioactivity expected at 100% labeling (cpm)	protein-bound radioactivity found (cpm)
Y227A	12	1100	95
Y229A	24	2200	200
Y229F	24	2200	2800
wild-type	15	1380	100

[a] The expected protein-bound radioactivity at 100% labeling was calculated on the basis that 1 mol of enzyme is converted with 1 mol of [4-^{14}C]oxaloacetate into the [^{14}C]carboxybiotin enzyme derivative. The molecular weight of oxaloacetate decarboxylase 117 300 was used. The reactions were performed in the presence of 10 mM NaCl. For details, see Experimental Procedures.

Table 3: Effect of OadB Mutations on Na^+ Binding Characteristics and pH Profiles of the Corresponding Oxaloacetate Decarboxylases

mutation	halfmaximal activation by Na^+ (mM)	pH-optimum	half-time for OadB digestion[a] ($+Na^+/-Na^+$) (h)
wild-type	0.5	7.0	>24/12
N55A	1.2	6.5	nd
T148A	0.7	6.0	nd
T189A	1.2	6.0	nd
Q192L	3.6	5.5	nd
G197A	0.8	6.5−7.0	nd
G200A	0.7	nd	nd
G201A	2.3	6.0	nd
G204A	1.9	6.5	nd
T206A	0.8	6.0−6.5	nd
Y209A	1.7	5.5	nd
E217A	0.9	6.5	nd
Y227A	nd	nd	>24/12
Y227C	1.1	7.5	nd
Y227F	1.0	6.5−7.0	>24/12
Y229A	nd	nd	>24/12
Y229F	nd	nd	>24/12
Q237A	0.7	6.0	nd
D282A	0.8	7.0	nd
C291E	nd	nd	>24/12
T318A	2.7	6.5	nd
T354A	0.9	6.5	nd
S419A	1.1	7.5	nd

[a] Half-time for digestion of OadB by trypsin in the presence of 50 mM NaCl ($+Na^+$) or in the absence of Na^+ ($-Na^+$). nd = not determined.

Effect of OadB Mutations on Na^+-Binding Characteristics and pH Profiles. As reported previously, OadB is specifically protected from tryptic hydrolysis at 20−50 mM Na^+ (*13*, *27*). Under our conditions, the halftime for tryptic digestion

of wild-type OadB was 12 h in the absence of Na^+ and >24 h in the presence of 50 mM NaCl. It has also been noticed that the catalytically inactive OadB mutants G377A, S382C, S382E, S382N, or S382Q yielded halftimes for tryptic digestion of about 1 h, indicating structures for these OadB variants that are more susceptible to proteolysis (*15*). The characteristics of the OadB mutants Y227A, Y227F, Y229A, Y229F, and C291E with respect to tryptic hydrolysis in the presence or absence of Na^+ ions were similar to the wild-type enzyme. Hence, these variants not only adopt a structure, which is rather resistant to hydrolysis by trypsin, but they also retain the Na^+-binding sites which, when occupied, further protect OadB from tryptic digestion.

The Na^+-binding affinities were also analyzed by the Na^+ activation profiles for oxaloacetate decarboxylation. The results of Table 3 indicate that in all mutants the Na^+ concentration yielding half-maximal activation increased to various extends compared to the wild-type, most significantly in the Q192L, G201A, and T318A mutants, where the increase was between seven and 5-fold. For most mutant decarboxylases, the pH optimum was between 6.5 and 7.5 and, thus, similar to the wild-type enzyme. Exceptions are the Q192L and Y209A mutants, which have a pH optimum of 5.5.

The mutants were further characterized by their ability to complement the Na^+/H^+ antiporter deletion strain *E. coli* EP432 (*15*). Due to the lack of both Na^+/H^+ antiporters NhaA and NhaB, the cellular Na^+ concentration reaches toxic levels at elevated Na^+ concentrations in the growth medium, and *E. coli* EP432 does not grow (*17*). Recently, we have shown that the ability of this antiporter deletion strain to grow on glucose mineral medium containing 360 mM NaCl is restored upon transformation with the genes for a functional oxaloacetate decarboxylase Na^+ pump, but not with genes encoding mutant enzymes with no or very little catalytic acitivities (*15*). It has also been verified that appropriate transformants of *E. coli* EP432 synthesized a functional oxaloacetate decarboxylase Na^+ pump. On the basis of the correlation between growth of *E. coli* EP432 at elevated Na^+ concentrations and the synthesis of a functional oxaloacetate decarboxylase in these cells, we attribute the growth phenotype to an extrusion of toxic internal Na^+ concentrations by the oxaloacetate decarboxylase Na^+ pump. The results given in Table 1 show growth at elevated Na^+ concentrations for *E. coli* EP432 transformants synthesizing the OadB mutants with specific oxaloacetate decarboxylase activities of more than 2 units/mg protein. The Y227A, Y229A, and Y229F mutants, on the other hand, having specific activities of less than 0.5 units/mg protein, were unable to complement *E. coli* EP432 for growth at elevated Na^+ concentrations, which indicates that the Na^+ pump function is either impaired or very low.

DISCUSSION

In the effort to determine all functionally important amino acid residues on the oxaloacetate decarboxylase β-subunit (OadB), we have now mutagenized another 20 polar and/or conserved amino acid residues within putative integral membrane regions. Oxaloacetate decarboxylases with these OadB mutations were synthesized in *E. coli* and could be purified as the three-subunit complexes, irrespective of whether Na^+ ions were present or absent. Hence, these mutations do not affect the assembly or stability of the enzyme complex. The only exception is the βC291E mutant, from which the $\alpha\beta\gamma$ complex could only be isolated in the presence of 0.5 M NaCl, while in the absence of Na^+, the enzyme dissociated into the $\alpha-\gamma$ subcomplex and the free β-subunit during chromatography on the monomeric avidin-Sepharose column. According to recent topology analysis, C291 is located within putative transmembrane helix V near the periplasmic surface (*11*). As C291 is not conserved, it is unlikely to play a universal role in complex formation among the related enzymes. We rather assume a conformational change in OadB due to the C291E mutation through which the three-subunit complex becomes destabilized. It has already been noted that in the presence of elevated Na^+ concentrations (>20 mM) OadB changes its conformation and becomes more resistant to tryptic digestion (*13*, *27*). Possibly, the protease-resistant conformation of OadB, adopted at elevated Na^+ concentrations, also contributes to the stability of the complex. Hence, the enzyme complex which is destablized by the C291E mutation, dissociates in the absence of Na^+, but keeps together in the presence of 0.5 M NaCl. The glutaconyl-CoA decarboxylase β-subunit from *Acidaminococcus fermentans* contains a cysteine residue at position 299 (OadB numbering) in the loop connecting helices V and VI. This particular cysteine residue was modified by *N*-ethylmaleinimide, and NaCl (>10 mM) specifically protected from the modification, indicating a Na^+-induced conformational change within this area of the molecule (*3*). However, as the loop between helices V and VI is located in the periplasm, where Na^+ binding is not expected to take place, it is likely that the Na^+-induced burying of C299 marks a more global conformational change that also includes other parts of the protein.

In most of the OadB mutants investigated here, the specific oxaloacetate decarboxylase activity was significantly affected. As we have mutated conserved residues that may contribute to the optimal function of the enzyme, this result is not unexpected. It is noteworthy that all mutant decarboxylases except those with the tyrosine mutations described below were functional Na^+ pumps. Hence, none of the mutations investigated here led to an uncoupled phenotype of the decarboxylase. On the basis of our recent proposal for the coupling mechanism, mutations leading to an uncoupled oxaloacetate decarboxylase are not to be expected: in this proposal, the proton consumed in the decarboxylation of carboxybiotin and the two Na^+ ions pumped traverse the membrane within opposite directions (*12*). Furthermore, S382 in the center of the membrane alternatively acts as a binding site for Na^+ or for the catalytic proton. For the hydroxyl proton of S382 to be displaced and consumed in the decarboxylation reaction, Na^+ binding is mandatory (*15*). According to this model, any mutation that affects the Na^+-binding characteristics of S382 or the Na^+ access channels to this site will automatically affect the displacement of H^+ from S382 and, as a consequence, the decarboxylation of carboxybiotin. It is for these reasons that we do not anticipate an uncoupling of the decarboxylation event from the translocation of Na^+ ions.

Transmembrane helix IV contains two universally conserved tyrosine residues close to the center of the membrane, which are separated by a single serine or leucine residue.

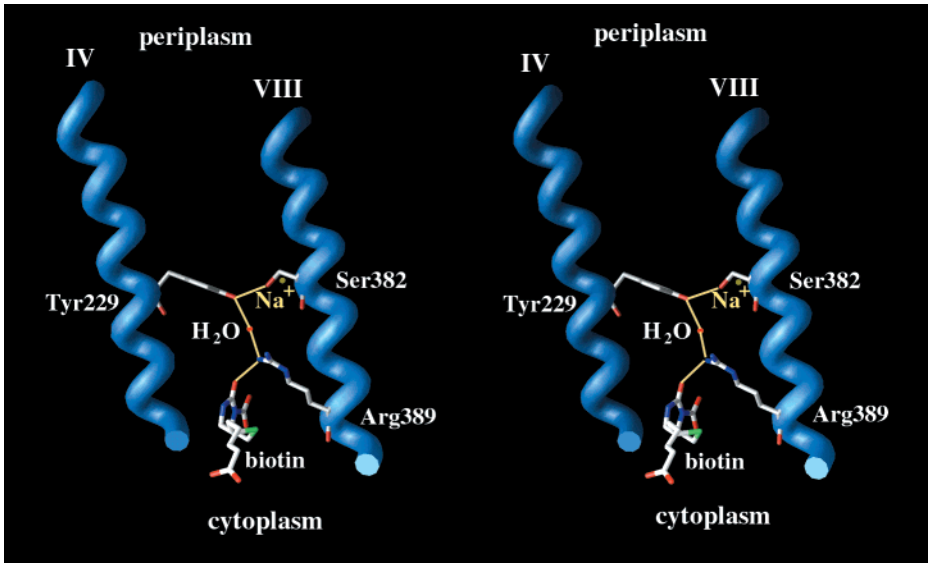

FIGURE 4: Model (stereoview) for the proton translocation network within the cytoplasmic channel of OadB. Na^+ entering through this channel displaces a proton from the hydroxyl side chain of S382. This leads to the rearrangement of hydrogen bonds in the network which includes S382, Y229, H_2O, R389, and carboxybiotin with ultimately delivering a proton to the carboxybiotin, where it is consumed in the decarboxylation reaction.

Decarboxylase with a Y227A mutation was nearly inactive, but in enzyme specimens with the Y227F or Y227C mutation, approximately 25% of the wild-type decarboxylase activity was retained, indicating that Y227 is not an indispensable residue for function. In contrast, enzyme with a Y229F mutation was completely inactive and that with a Y229A mutation retained only traces of activity. Therefore, Y229 appears to be an important residue for the function of the enzyme. Unlike to the putative Na^+-binding residues D203 and S382 (*12*, *15*), neither Y227 nor Y229 appear to participate in Na^+ binding, since Na^+ protection from tryptic hydrolysis was similar in the wild-type OadB and in the Y227A, Y227F, Y229A, or Y229F mutants (Table 3).

We do not anticipate a mere structural role for Y229, because this would not be compatible with the complete knockout of catalytic activity upon replacing the phenol by a phenyl ring and with the retention of some activity in the less conservative Y229A mutant. The hydroxyl group of Y229 could rather be part of hydrogen-bonded network, allowing efficient transfer of the proton required for catalysis from S382 in the middle of the membrane to carboxybiotin at the cytoplasmic surface. Here, the proton is consumed in the decarboxylation reaction. R389 and bound water molecules might also be involved in the network (see below, Figure 4). If Y229 is indeed an essential component of the proton channel leading from S382 to carboxybiotin, the Y229F mutant should be inactive. This supposition is in accord with the evidence. The small residual activity observed with the Y229A mutant might be explained by the smaller side chain of alanine as compared to phenylalanine. This could provide sufficient space for a water molecule to contact S382, thereby serving as a substitute for Y229 in the proton translocation network. Precedence for a hydrogen-bonded network containing tyrosines was found in the crystal structure of bacteriorhodopsin (*28*). Here, an aspartate, an arginine, two tyrosines, and a water molecule are included, and it was speculated that the network may account for the unusually low p*K* (<2) of the aspartate 212 involved.

A hydrogen-bonded network may also exist within the cytoplasmic portion of OadB where it may account for the proton translocation pathway from S382 in the center of the membrane to the carboxybiotin near the cytoplasmic surface. This network could involve S382, Y229, R389, and carboxybiotin. Molecular modeling (Figure 4) indicated that these side chains, being contributed by helices IV and VIII, could be within hydrogen-bonding distances, provided a water molecule bridges Y229 and R389. Importantly, S382 and R389 are exposed to the same surface of helix VIII. On the basis of the phenotype of several different mutants in this region, it has already been proposed that the hydroxyl group of S382 switches between the deprotonated, Na^+-bound and the protonated state and that R389 facilitates the deprotonation of S382 (*15*). Compelling results along these lines are the observation that the S382D mutant is catalytically active, while S382N is inactive and that the R389K mutant resembles the wild-type, whereas the R389L mutant has low catalytic activity combined with an increase of the pH optimum by about 3 pH units. Our present results suggest that Y229 is another residue that is indispensable for the decarboxylation of the carboxybiotin. For these reasons, we extend our previous model (*15*) and include Y229 in the hydrogen-bonded network that links S382 to carboxybiotin (Figure 4). R389 and carboxybiotin may have similar functions as the catalytic histidine and aspartate residues in serine proteases, i.e., to reduce the p*K* of S382. It is conceivable, therefore, that Na^+ approaching S382 through the cytoplasmic channel can displace the proton from the hydroxyl side chain of S382, especially as the newly formed ion pair within the hydrophobic environment of the membrane would be thermodynamically more favorable than the presence of a Na^+ ion with an unbalanced positive charge. This displacement might induce the rearrangement of hydrogen bonding within the network to ultimately deliver a proton to carboxybiotin to catalyze the immediate decarboxylation of this acid-labile compound. The reaction may initiate a conformational change by which the cytoplasmic

channel closes and a periplasmic channel opens. The two Na^+ ions bound to the D203 and S382 including sites (*15*) could then be released through this channel into the periplasmic compartment. To displace the Na^+ form S382, a periplasmic proton penetrating through the channel must restore the hydroxyl group of S382 because an uncompensated negative charge would not be tolerated near the center of the membrane for electrostatic reasons. For the proton to reach this deeply embedded membrane position, it could first bind to D203 near the periplasmic surface, thereby releasing the first Na^+ ion, and could subsequently be transmitted to S382 with the release of the second Na^+ ion. An obligatory requirement of D203 and S382 in the proton translocation pathway is compatible with the observation that the decarboxylase activity is completely abolished if either of these residues is mutated (*12*, *15*). The proposed mechanism is also compatible with the observation that the translocation of 2 Na^+ ions from the cytoplasm into the periplasm is coupled to the consumption of a periplasmically derived proton in the decarboxylation reaction (*12*).

SUPPORTING INFORMATION AVAILABLE

Table listing the primers used for mutagenesis of the β-subunit. This material is available free of charge via the Internet at http://pubs.acs.org.

REFERENCES

1. Dimroth, P. (1997) *Biochim. Biophys. Acta 1318*, 11−51.
2. Dimroth, P., and Schink, B. (1998) *Arch. Microbiol. 170*, 69−77.
3. Braune, A., Bendrat, K., Rospert, S., and Buckel, W. (1999) *Mol. Microbiol. 31*, 473−487.
4. Schwarz, E., Oesterhelt, D., Reinke, H. Beyreuther, K., and Dimroth, P. (1988) *J. Biol. Chem. 263*, 9640−9645.
5. Lauβermair, E., Schwarz, E., Osterhelt, D., Reinke, H., Beyreuther, K., and Dimroth, P. (1989) *J. Biol. Chem. 264*, 14710−14715.
6. Woehlke, G., Lauβermair, E., Schwarz, E., Oesterhelt, D., Reinke, H., Beyreuther, K., and Dimroth, P. (1992) *J. Biol. Chem. 267*, 22804−22805.
7. Bott, M., and Dimroth, P. (1994) *Mol. Microbiol. 14*, 347−356.
8. Bott, M., Meyer, M., and Dimroth, P. (1995) *Mol. Microbiol. 18*, 533−546.
9. Bott, M. (1997) *Arch. Microbiol. 167*, 78−88.
10. Dimroth, P., and Thomer, A. (1986) *Eur. J. Biochem. 156*, 157−162.
11. Jockel, P., Di Berardino, M., and Dimroth, P. (1999) *Biochemistry 38*, 13461−13472.
12. Di Berardino, M., and Dimroth, P. (1996) *EMBO J. 15*, 1842−1849.
13. Dimroth, P., and Thomer, A. (1992). *FEBS Lett. 300*, 67−70.
14. Di Berardino, M., and Dimroth, P. (1995) *Eur. J. Biochem. 231*, 790−801.
15. Jockel, P., Schmid, M., Steuber, J., and Dimroth, P. (2000) *Biochemistry 39*, 2307−2315.
16. Yanish-Perron, C., Vieira, J., and Messing, J. (1995) *Gene 33*, *103−119*.
17. Pinner, E., Kolter, Y., Padan, E., and Schuldiner, S. (1993) *J. Biol. Chem. 268*, 1729−1734.
18. Dunn, J. J., and Studier, F. W. (1983) *J. Mol. Biol. 219*, 45−59.
19. Sambrook, J., Fritsch, E. F., and Maniatis, T. (1989) *Molecular cloning: A laboratory manual*, 2nd ed., Cold Spring Harbor Laboratory, Plainview, NY.
20. Sanger, F., Nicklen, S., and Coulson, A. R. (1977) *Proc. Natl. Acad. Sci. U.S.A.* 74, 5463−5467.
21. Dimroth, P. (1986) *Methods Enzymol. 125*, 530−540.
22. Bradford, M. M. (1979) *Anal. Biochem. 72*, 248−251.
23. Smith, P. K., Krohn, R. I., Hermanson, G. T., Mallia, A. K., Gartner, F. H., Provenzano, M. D., Fujimoto, E. K., Goeke, N. M., Olson, B. J., and Klenk, D. C. (1985) *Anal. Biochem. 150*, 76−85.
24. Sack, J. S. (1988) *J. Mol. Graphics 6*, 224−225.
25. Pugliese, L., Coda, A., Malcovati, M., and Bolognesi, M. (1993) *J. Mol. Biol. 231*, 698−710.
26. Dimroth, P., and Thomer, A. (1988) *Eur. J. Biochem. 175*, 175−180.
27. Dimroth, P., and Thomer, A. (1983) *Eur. J. Biochem. 137*, 107−112.
28. Luecke, H., Richter, H.-T., and Lanyi, J. K. (1998) *Science 280*, 1934−1937.

BI992817E